

ABSTRACT

Title of Dissertation: **NONLINEAR PULSE PROPAGATION
THROUGH AN OPTICAL FIBER:
THEORY AND EXPERIMENT**

Bhaskar Khubchandani
Doctor of Philosophy, 2004

Dissertation Directed by: **Professor Rajarshi Roy**
Department of Physics

NOTE: Proquest no longer requires a limit to the length of the Abstract.

Pulse propagation through optical fibers is studied for two different phenomena: (i) the evolution of four-wave-mixing and (ii) the interplay between self- and cross-phase modulation for ultra-short pulses in a polarization maintaining fiber.

For the four-wave-mixing case, we present the results of a study of the dynamical evolution of multiple four-wave-mixing processes in a single-mode optical fiber with spatially and temporally δ -correlated phase noise. A nonlinear Schrödinger equation (NLSE) with stochastic phase fluctuations along the length of the fiber is solved using the Split-Step Fourier method. Good agreement is obtained with previous experimental and computational results based on a truncated-ODE model in which stochasticity was seen to play a key role in determining the nature of the dynamics. The full NLSE allows for simulations with high frequency resolution (60 MHz) and frequency span (16 THz) compared to the truncated ODE model (300 GHz and 2.8 THz),

thus enabling a more detailed comparison with observations. Fluctuations in the refractive index of the fiber core are found to be a possible source for this phase noise. It is found that index fluctuations as small as 1 part per billion are sufficient to explain observed features of the evolution of the four-wave-mixing sidebands. These measurements and numerical models thus may provide a technique for estimating these refractive index fluctuations which are otherwise difficult to measure.

For the case of self- and cross-phase modulation, the evolution of orthogonal polarizations of asymmetric femtosecond pulses (810 nm) propagating through a birefringent single-mode optical fiber (6.9 cm) is studied both experimentally (using GRENOUILLE) and numerically (using a set of coupled NLSEs). A linear optical spectrogram representation is derived from the electric field of the pulses and juxtaposed with the optical spectrum and optical time-trace. The simulations are in good qualitative agreement with the experiments. Input temporal pulse asymmetry is found to be the dominant cause of output spectral asymmetry. The results indicate that it is possible to modulate short pulses both temporally and spectrally by passage through polarization maintaining optical fibers with specified orientation and length.

NONLINEAR PULSE PROPAGATION THROUGH
AN OPTICAL FIBER: THEORY AND EXPERIMENT

by

Bhaskar Khubchandani

Dissertation submitted to the Faculty of the Graduate School of the
University of Maryland, College Park in partial fulfillment
of the requirements for the degree of
Doctor of Philosophy
2004

Advisory Committee:

Professor Rajarshi Roy, Chair/Advisor
Dr. Parvez N. Guzdar, Co-Advisor
Professor Robert W. Gammon
Professor Thomas M. Antonsen, Jr.
Professor Edward Ott

© Copyright by
Bhaskar Khubchandani
2004

Preface

If needed.

Foreword

If needed.

Dedication

If needed.

Acknowledgments

I owe my gratitude to all the people who have made this thesis possible and because of whom my graduate experience has been one that I will cherish forever.

First and foremost I'd like to thank my advisor, Professor Rajarshi Roy for giving me an invaluable opportunity to work on challenging and extremely interesting projects over the past four years. He has always made himself available for help and advice and there has never been an occasion when I've knocked on his door and he hasn't given me time. It has been a pleasure to work with and learn from such an extraordinary individual.

I would also like to thank my co-advisor, Dr. Parvez Guzdar. Without his extraordinary theoretical ideas and computational expertise, this thesis would have been a distant dream. Thanks are due to Professor Robert Gammon, Professor Edward Ott and Professor Thomas Antonsen for agreeing to serve on my thesis committee and for sparing their invaluable time reviewing the manuscript.

My colleagues at the nonlinear optics laboratory have enriched my graduate life in many ways and deserve a special mention. David DeShazer helped me start-off by rewriting the basic simulation code in a user-friendly format. Christian Silva provided help by setting up the GRENOUILLE apparatus and performing some of the simulations. My interaction with Rohit Tripathi, Ryan McAllister, Vasily Dronov, Min-Young Kim, Elizabeth Rogers, William Ray, Jordi Garcia Ojalvo, Riccardo Meucci, Atsushi Uchida, and Fabian Rogister has been very fruit-

ful. I'd also like to thank Wing-Shun Lam and Benjamin Zeff for providing the LaTeX style files for writing this thesis.

I would also like to acknowledge help and support from some of the staff members. Donald Martin's technical help is highly appreciated, as is the computer hardware support from Edward Condon, LaTeX and software help from Dorothea Brosius and purchasing help from Nancy Boone.

I owe my deepest thanks to my family - my mother and father who have always stood by me and guided me through my career, and have pulled me through against impossible odds at times. Words cannot express the gratitude I owe them. I would also like to thank Dr. Mohan Advani, Dr. Vasudeo Paralikar and Dr. Vinod Chaugule who are like family members to me.

My housemates at my place of residence have been a crucial factor in my finishing smoothly. I'd like to express my gratitude to Sivasankar Pandeti, Jayakumar Patil, Amit Trehan and Punyaslok Purakayastha for their friendship and support.

I would like to acknowledge financial support from the Office of Naval Research (ONR), Physics, for all the projects discussed herein.

It is impossible to remember all, and I apologize to those I've inadvertently left out.

Lastly, thank you all and thank God!

Table of Contents

Preface	ii
Foreword	iii
Dedication	iv
Acknowledgements	v
Table of Contents	vii
List of Tables	ix
List of Figures	x
List of Abbreviations	xi
Chapter 1: Introduction	1
1.1 Source of Nonlinearity in an Optical Fiber	1
1.2 Physics of Pulse Propagation	3
1.3 Numerical Pulse Propagation	7
1.4 Experimental Pulse Diagnostics	7
1.5 Group Velocity Dispersion	8
1.6 Self-Phase Modulation	9
1.7 Four-wave-mixing	9
1.8 Cross-Phase Modulation	10
1.9 Stimulated Inelastic Scattering	11
1.10 Outline of Thesis	12
1.11 Theorems	14
1.12 Axioms	14
1.13 Tables	14
1.13.1 Adding Extra Space between Text and Horizontal Lines	15
1.14 Figures	17
1.14.1 Numbering Figures	23
1.15 Short Titles	23
1.16 Figures on Text Page	24
1.17 Wrapping Text around Figure	24
1.18 LaTeX – A Typesetting Program	26

1.19 Using Bibtex	26
1.20 Using Natbib	27
1.21 APS Physical Review Style and Notation Guide	28
Bibliography	29

List of Tables

1.1	Short title	14
1.2	Table with Extra Space between the Text and Horizontal Lines.	15

List of Figures

1.1	Figure with caption indented	17
1.2	Schematic illustrating receding horizon control.	20
1.3	Figure placed landscape on page	22
1.4	Creating subfigures in \LaTeX	23
1.5	Schematic illustrating receding horizon control.	25
1.6	Text wrap around figure. Text wrap around figure. Text wrap around figure. Text wrap around figure. Text wrap around figure. Text wrap around figure. Text wrap around figure.	25

List of Abbreviations

AAA	Antiaircraft artillery
ABCCC	Airborne Battlefield Command and Control Center
AEHF	Advanced Extremely High Frequency
AGM	Air-to-ground guided missile
AIT	Assembly, Integration, and Testing
AOR	Area of Responsibility
APAM	Anti-personnel, anti-material
ASOC	Air Support Operations Center
ATACM	Army Tactical Missile System
ATO	Air Tasking Order
AWACS	Airborne Warning and Control System
BAT	Brilliant Ani-Armor Submunition
BDA	Bomb-damage assessment
BFT	Blue Force Tracking
BLOS	Beyond Line-of-Sight
BMD	Ballistic Missile Defense
C ³	Command, Control, and Communications
CAFMS	Computer-aided Force Management System
CALCM	Conventional Air-Launched Cruise Missile
CBU	Cluster Bomb Unit
CCAFS	Cape Canaveral Air Force Station
CENTAF	CENTCOM's Air Force component
CENTCOM	U.S. Central Command
CINC	Commander-in-Chief
CONUS	Continental United States
DAGR	Defense Advanced GPS Receiver
DMA	Defense Mapping Agency
DOD	Department of Defense
DOP	Dilution of Precision
DOT	Department of Transportation
DSMAC	Digital Scene Mapping Area Correlator

EFOG-M	Enhanced Fiber Optic Guided Missile
FAA	Federal Aviation Administration
FLIR	Forward-looking infrared
GAM	Global Positioning System Aided Munition
GPS	Global Positioning System
GWAPS	Gulf War Air Power Survey
HARM	High-Speed Antiradiation Missile
HEO	Highly Elliptical Orbit
IADS	Integrated Air Defense System
ICBM	Inter-Continental Ballistic Missile
INS	Inertial navigation system
IIR	Imaging infrared
IR	Infrared
ISR	Intelligence, Surveillance, and Reconnaissance
JDAM	Joint Direct Attack Munition
JFC	Joint Force Commander
JSOW	Joint Standoff Weapon
LANTIRN	Low-Altitude Navigation and Targeting Infrared for Night System
LEO	Low Earth Orbit
LGB	Laser-guided bomb
MAJIC	Microsatellite Area-Wide Joint Information Communication
MARCENT	CENTCOM's Marine component
MARS	Mid-Atlantic Regional Spaceport
MLRS	Multiple Launch Rocket System
MUOS	Mobile User Objective System
NASA	National Aeronautics and Space Administration
NAVCENT	CENTCOM's Navy component
NPOESS	National Polar-Orbiting Operational Environmental Satellite System
ORS	Operationally Responsive Space
ORSO	Operationally Responsive Space Office

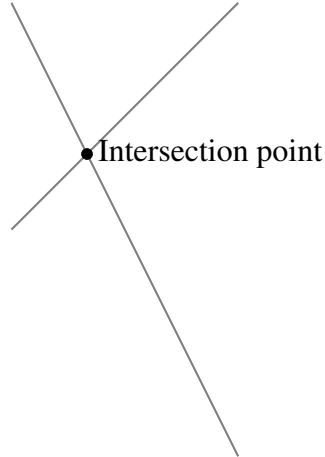
PDOP	Position Dilution of Precision
PGM	Precision-guided munition
P ³ I	Preplanned Product Improvement
PnP	Plug and Play
PnPSat	Plug and Play Satellite
PPS	Precise Positioning Service
RCS	Radar cross section
SA	Situational Awareness
SADARM	Sense and Destroy Armor Munition
SAM	Surface-to-air missile
SAR	Synthetic aperture radar
SBIRS	Space Based Infrared System
SEAD	Suppression of enemy air defenses
SFW	Sensor Fuzed Weapon
SIGINT	Signal Intelligence
SLAM	Standoff Land Attack Missile
SLAM-ER	SLAM-Expanded Response
SpaceX	Space Exploration Technologies Corporation
SPS	Standard Positioning Service
TACC	Tactical Air Control Center
TACS	Tactical Air Control System
TACP	Tactical Air Control Party
TASM	Tomahawk Anti-Ship Missile
TBIP	Tomahawk Baseline Improvement Program
TERCOM	Terrain Contour Mapping
TFR	Terrain-following radar
TLAM	Tomahawk Land Attack Missile
USAF	U.S. Air Force
VAFB	Vandenberg Air Force Base
WGS	Wideband Global SATCOM

Chapter 1: Introduction

1.1 Source of Nonlinearity in an Optical Fiber

The response of any dielectric to light becomes nonlinear for intense electromagnetic fields. Standard optical fibers are made of fused silica which is a dielectric. The total polarization \mathbf{P} is nonlinear in the electric field \mathbf{E} and is given by [1-5]

The figure below was originally made using the TIKZ package.



$$\mathbf{P} = \epsilon_0 \left(\chi^{(1)} : \mathbf{E} + \chi^{(2)} : \mathbf{E}\mathbf{E} + \chi^{(3)} : \mathbf{E}\mathbf{E}\mathbf{E} + \dots \right), \quad (1.1)$$

where ϵ_0 is the permittivity of free-space, and $\chi^{(j)}$ is the j -th order susceptibility of the dielectric. The linear susceptibility $\chi^{(1)}$ represents the dominant contribution to \mathbf{P} and its effects are included through the refractive index $n(\omega)$ and the attenuation coefficient $\alpha(\omega)$. $\chi^{(2)}$ is responsible

for nonlinear effects such as sum-frequency generation and second harmonic generation [?, ?]. Fused silica does not manifest these effects as it is centro-symmetric [?]. Hence, the dominant nonlinear contribution to \mathbf{P} is due to $\chi^{(3)}$ which results in effects such as third harmonic generation, four-wave-mixing, self- and cross-phase modulation. The cubic nonlinearity results in an intensity dependent refractive index

$$122 \quad 23333$$

$$1114 \quad 14444$$

$$\tilde{n}(\omega, |E|^2) = n(\omega) + n_2|E|^2, \quad (1.2)$$

where $n(\omega)$ is the linear part given by the Sellmeyer equation which takes into account the resonance frequencies (ω_j) of fused silica [?, ?],

$$n^2(\omega) = 1 + \sum_{j=1}^m \frac{B_j \omega_j^2}{\omega_j^2 - \omega^2} \quad (1.3)$$

and n_2 is given by

$$n_2 = \frac{3}{8n} \text{Re}(\chi_{xxxx}^3) \quad (1.4)$$

for an optical wave assumed to be linearly polarized along one of the axes of a polarization maintaining fiber. The tensorial nature of $\chi^{(3)}$ needs to be considered for the case in which the light is not polarized along one of the fiber axes.¹

The following is an equation array to ensure the long equation does not go outside the

¹This is my footnote. I started playing the piano when I was eight years old. This is my footnote. I started playing the piano when I was eight years old. This is my footnote. I started playing the piano when I was eight years old. This is my footnote. I started playing the piano when I was eight years old.

margins.

$$\begin{aligned}
W &= \int d^3\mathbf{r} \left[\sum_s \left(\int d^3\mathbf{v} \frac{T_{0s} \langle h_s^2 \rangle \mathbf{r}}{2F_{0s}} - \frac{q_s^2 \varphi^2 n_{0s}}{T_{0s}} \right) + \frac{|\delta\mathbf{B}|^2}{8\pi} \right] \\
&= \int d^3\mathbf{r} \left(\sum_s \int d^3\mathbf{v} \frac{T_{0s} \delta f_s^2}{2F_{0s}} + \frac{|\delta\mathbf{B}|^2}{8\pi} \right).
\end{aligned} \tag{1.5}$$

The experimentally measured value of n_2 for fused silica ranges from $2.2-3.4 \times 10^{-20} \text{ m}^2/\text{W}$, which is small compared to most other nonlinear media by at least 2 orders of magnitude [?]. Despite this, nonlinear effects are easily observed for silica fibers for relatively low input power levels due to the fact that the effective fiber core areas are small and the fiber losses are low. Single mode fibers (those which propagate a single transverse mode of light for a given wavelength) have effective fiber core diameters of the order of $5\mu\text{m}$ thus causing the light intensities within the fiber to be large despite the smallness of the input power. The low loss in the fiber ($<10 \text{ dB/km}$) allows one to use long fibers to observe nonlinear phenomena.

1.2 Physics of Pulse Propagation

Mathematically speaking, in the classical limit, pulse propagation in an optical fiber is governed by Maxwell's equations [?, ?],

$$\begin{aligned}
\vec{\nabla} \times \vec{E} &= -\frac{\partial \vec{B}}{\partial t} \\
\vec{\nabla} \times \vec{H} &= \vec{J} + \frac{\partial \vec{D}}{\partial t} \\
\vec{\nabla} \cdot \vec{D} &= \rho_f \\
\vec{\nabla} \cdot \vec{B} &= 0,
\end{aligned} \tag{1.6}$$

where \vec{E} and \vec{H} are electric and magnetic field vectors, and \vec{D} and \vec{B} are electric and magnetic flux densities, respectively. \vec{J} is the current density and ρ_f is the free charge density.

This is the second equation array.

$$\begin{aligned} W &= \int d^3r \left[\sum_s \left(\int d^3v \right) \frac{T_s \langle h_s^2 \rangle_r}{2F_{0s}} \right] + \frac{|\delta B|^2}{8\pi} \\ &= \int d^3 \end{aligned} \quad (1.7)$$

Under the following assumptions [?] -

- (a) there are no free charges ($\vec{J} = \rho_f = 0$), a good approximation for an optical fiber,
- (b) the medium is non-magnetic ($\vec{M} = 0$), which an optical fiber is,
- (c) the wavelength of light propagated is away from any material resonances (0.5 - 2 μm), the results described in this thesis lie in this wavelength range, i.e., the results presented in Chap. 2 and Chap. 3 lie in the 600-700 nm regime and the results presented in Chap. 4 lie in the 800 nm regime,
- (d) the electric-dipole approximation is valid, due to which the second-order parametric processes such as three-wave-mixing and second harmonic generation can be neglected (in practice they do occur because of quadrupole and magnetic-dipole effects but with a very low efficiency),
- (e) the medium only responds locally, which is a valid approximation for the projects considered herein,
- (f) the nonlinear polarization \vec{P}_{NL} can be taken as a perturbation to the total induced polar-

ization \vec{P} , which is justified as the nonlinear effects are relatively weak for the results presented in this thesis,

- (g) only 3rd order nonlinear effects need to be taken into account, which is valid up to 5th order in \mathbf{E} since the 2nd and 4th order effects are absent due to the centrosymmetric nature of the disordered liquidlike state of fused silica,
- (h) the imaginary part of the dielectric constant $\epsilon(\omega)$ is small compared to the real part (low loss, which is a good approximation for the wavelength regimes and fiber lengths considered here),
- (i) the wavelength of light is higher than the cutoff wavelength of the fiber so that the single transverse mode condition is satisfied (or else there would be multimode propagation and nonuniform modal dispersion would have to be taken into account),
- (j) the optical fiber is polarization maintaining and the light pulse is traveling along one of the 2 principal axes of the fiber, a very good approximation for the results of Chap. 2, and Chap. 3, in the case of Chap. 4, this approximation is relaxed as the incident light travels along both axes of the fiber, thus requiring a set of two coupled NLSEs for simulation, one for each axis,
- (k) the slowly varying envelope approximation is valid, i.e., $\Delta\omega/\omega_0 \ll 1$ where $\Delta\omega$ is the spectral width of the pulse spectrum which is centered at ω_0 , this approximation is valid for the studies considered in Chap. 2 and Chap. 4, in Chap. 3, the Raman Stokes wave is considered as a separate slowly varying envelope from the pump wave, as the two taken together would not satisfy this condition,

- (l) the nonlinear response of the medium is instantaneous, an approximation valid for pulse widths greater than ~ 70 fs, which amounts to neglecting the contribution of molecular vibrations to $\chi^{(3)}$ (the Raman effect), which have been included in the study presented in Chap. 4 since the pulse width was ~ 140 fs.

The propagation of the slowly varying envelope $A(z,t)$ of a light pulse along an optical fiber is governed by the nonlinear partial differential equation [?] -

$$\frac{\partial A}{\partial z} + \beta_1 \frac{\partial A}{\partial t} + \frac{i\beta_2}{2} \frac{\partial^2 A}{\partial t^2} = i\gamma |A|^2 A, \quad (1.8)$$

where $v_g = 1/\beta_1$ is the group velocity of the pulse, β_2 is the group velocity dispersion coefficient, and γ is the nonlinearity coefficient given by

$$\gamma = \frac{n_2 \omega_0}{c A_{eff}}. \quad (1.9)$$

Here ω_0 is the central angular frequency of the pulse and A_{eff} , the effective core area of the fiber.

Under transformation to a frame of reference moving at the group velocity of the pulse, the above equation takes the form of the so-called ‘nonlinear Schrödinger equation’ (NLSE), i.e.,

$$\frac{\partial A}{\partial z} + \frac{i\beta_2}{2} \frac{\partial^2 A}{\partial \tau^2} = i\gamma |A|^2 A, \quad (1.10)$$

where

$$\tau = t - \frac{z}{v_g} \quad (1.11)$$

is time measured in a frame of reference moving at the group velocity v_g of the pulse.

1.3 Numerical Pulse Propagation

The NLSE, like most nonlinear partial differential equations, is not amenable to analytical solution except in certain special cases where the inverse scattering transform can be used [?]. Thus a numerical approach is necessary for understanding the physics of phenomena governed by the NLSE. The numerical methods available can be classified as finite-difference techniques and pseudo-spectral techniques. Usually pseudo-spectral methods are an order of magnitude faster, the most popular method being the Split-Step Fourier Method (SSFM) [?, ?, ?]. The speed of the SSFM can be partly attributed to the use of the finite fast-Fourier transform (FFT) algorithm [?]. For an algorithmic description of the SSFM the reader is referred to Chap. 2, Sec. 2. Therein is also described an unconditionally stable scheme for including linear multiplicative noise into the SSFM without disturbing the conservative properties of the NLSE. In the projects described in Chap. 3, simulations were carried out using a combination of the SSFM and finite difference schemes. The SSFM is also used to arrive at the simulated results described in Chap. 4.

1.4 Experimental Pulse Diagnostics

With the advent of frequency resolved optical gating (FROG) [?, ?, ?], it has become possible to not only measure the optical spectrum and optical time trace of a light pulse but to measure the full electric field envelope (intensity and phase) of the light pulse. The two fields of nonlinear fiber optics and frequency resolved optical gating (FROG) are yet to undergo cross pollination to their fullest potential since the inception of FROG 10 years ago. This novel experimental

technique adds new dimensions to pulse measurement techniques, one of which is the ability to measure how asymmetric a pulse is, i.e., measure its skewness, kurtosis and all higher order moments. Asymmetric pulse propagation is a subject of interest in Chap. 4, where a highly simplified version of FROG [?] is used to measure pulse characteristics before and after a fiber.

1.5 Group Velocity Dispersion

Group velocity dispersion [?] (GVD) involves the temporal broadening of a pulse as it propagates through an optical fiber. From the NLSE (Eq. 1.6) one can derive length scales relevant to linear dispersion ($L_D = T_0^2/\beta_2$) and nonlinearity ($L_{NL} = 1/\gamma P_0$). Here T_0 is the pulse width and P_0 is the peak power of the pulse. The regime in which the effects of GVD dominate and the effects of nonlinearity are negligible is given by -

$$\frac{L_D}{L_{NL}} = \frac{\gamma P_0 T_0^2}{|\beta_2|} \ll 1. \quad (1.12)$$

In this regime, optical pulses propagate as they undergo symmetric temporal broadening and linear chirping without any spectral broadening. The sign of the GVD parameter β_2 determines the sign of the induced chirp. If the input pulse is chirped, then it may undergo some initial pulse compression followed by temporal broadening. Unlike the second-order dispersion associated with GVD, third-order dispersion causes asymmetric temporal broadening with leading and trailing edges. It becomes important, when the operating wavelength is near the zero dispersion wavelength of the fiber (the wavelength at which $\beta_2=0$). GVD starts to limit optical fiber communication systems when consecutive pulses broaden so much that they start to overlap.

1.6 Self-Phase Modulation

Self-phase modulation [?] (SPM) is a phenomenon that leads to spectral broadening and modulation of optical pulses. In the absence of GVD, SPM induced spectral broadening occurs without change in the temporal pulse shape. The spectral broadening occurs as a consequence of an intensity dependent phase-shift. The project described in Chap. 2 has the property that $L_{NL} < L \ll L_D$, i.e., the nonlinear term representing SPM dominates. In the regime where both SPM and GVD are non-negligible (as in Chap. 4), phenomena qualitatively different from those described in this section and the previous section can occur. Both temporal and spectral broadening can occur simultaneously. In the regime of femtosecond pulse propagation (as in Chap. 4), GVD, third-order dispersion, intrapulse Raman scattering (discussed in Chap. 2) and higher order nonlinear effects have to be taken into account. If the input pulse is asymmetric, then SPM effects dominate over all other effects, as is observed in Chap. 3. In some cases SPM can lead to pulse compression, and in the anomalous dispersion regime ($\beta_2 < 0$), the balance between GVD and SPM can lead to soliton formation.

1.7 Four-wave-mixing

Four-wave-mixing (FWM) [?] is a parametric process involving the interaction between four photons at different frequencies. Two different kinds of four-wave-mixing processes are possible -

$$\omega_4 = \omega_1 + \omega_2 + \omega_3 \tag{1.13}$$

$$\omega_3 + \omega_4 = \omega_1 + \omega_2. \quad (1.14)$$

The former process results in third harmonic generation for the special case when $\omega_1 = \omega_2 = \omega_3$. Both processes require phase matching to occur, in order to be efficient. For the latter case, with the partial degeneracy of $\omega_1 = \omega_2$, it is relatively easy to satisfy the phase matching condition of

$$\Delta k = k_3 + k_4 - k_1 - k_2 = 0. \quad (1.15)$$

This process is of great interest to nonlinear dynamicists as the evolution of the FWM process could constitute a route to chaos further down-stream in the fiber. It is also of great interest to people working in the field of optical communication systems, as it can cause cross-talk between neighboring channels in a wavelength division multiplexing scheme of communication.

1.8 Cross-Phase Modulation

Cross-phase modulation (XPM) [?] occurs in optical fibers when two or more optical pulses having different central wavelengths propagate simultaneously inside a fiber, interacting through the fiber nonlinearity which couples the two pulses nonlinearly. The evolution of the two pulses depends on the group velocity mismatch between them by virtue of their being centered at different wavelengths, although this is a linear phenomenon. The group velocity mismatch also exists between light pulses traveling along orthogonal polarization axes of a fiber, and centered around identical wavelengths, since the slow axis and fast axis of the fiber have different group velocities. In this case, too, the two polarizations interact nonlinearly [?] through degenerate XPM (degenerate since the central wavelengths are the same). In the case of degenerate XPM the 2nd order

and higher dispersion parameters, and the nonlinear parameters (all of which depend only on the wavelength), are also the same unlike in general XPM. The effects of XPM are more pronounced when one of the pulses (the pump) has much higher power than the other (the probe). Otherwise, the effects of self-phase modulation (SPM) tend to dominate.

1.9 Stimulated Inelastic Scattering

Other nonlinear effects (apart from those due to the cubic $\chi^{(3)}$ nonlinearity) arise due to the interaction between the light traveling in the fiber and the fiber medium. Interactions between the light field and the vibrational levels of the fiber medium lead to stimulated Brillouin scattering (SBS) and stimulated Raman scattering (SRS). SRS and SBS were among the first nonlinear effects studied in optical fibers [?, ?, ?]. In a simple quantum mechanical picture [?] applicable to both SRS and SBS, a photon of the incident field (called the pump) is annihilated to create a photon at a lower frequency (belonging to the Stoke's wave) and a phonon to conserve energy and momentum. SBS involves an acoustic phonon whereas SRS involves an optical phonon, thus they have qualitatively different dispersion relations. SBS has a much lower threshold power and manifest itself through a backward propagating wave in contrast to SRS which can involve both forward and backward traveling waves. SBS has a maximum gain at a frequency 10 GHz [?] (down-shifted with respect to the pump) and requires a very narrow bandwidth pump to manifest itself. SRS, in contrast, has a maximum gain at a frequency 13 THz [?] downshifted with respect to the pump. For pulse-bandwidths larger than 13 THz, the phenomenon of Intrapulse Raman Scattering (IRS) manifests itself, involving a self-frequency shift within the pulse from higher frequency components to lower frequency components. Thus, SRS becomes more important for

shorter pulses (larger bandwidth) unlike SBS which nearly ceases to occur for pulses shorter than 10 ns. In both SRS and SBS, the optical fiber plays an active role in the nonlinear process, unlike the case of cross- and self-phase modulation, four-wave-mixing and third harmonic generation, where the fiber plays a passive role by mediating the interaction between several optical waves.

1.10 Outline of Thesis

In Chap. 2, we present the results of a computational study of the influence of stochasticity on the dynamical evolution of multiple four-wave-mixing processes in a single mode optical fiber with spatially and temporally δ -correlated phase noise. A generalized nonlinear Schrödinger equation (NLSE) with stochastic phase fluctuations along the length of the fiber is solved using the Split-step Fourier method (SSFM). Good agreement is obtained with previous experimental and computational results based on a truncated-ODE (Ordinary Differential Equation) model in which stochasticity was seen to play a key role in determining the nature of the dynamics. The full NLSE allows for simulations with high frequency resolution (60 MHz) and frequency span (16 THz) compared to the truncated ODE model (300 GHz and 2.8 THz, respectively), thus enabling a more detailed comparison with observations. A physical basis for this hitherto phenomenological phase noise is discussed and quantified.

In Chap. 3, we discuss the implications of spontaneous and stimulated Raman scattering on the project discussed in Chap. 2, namely, the dynamical evolution of stochastic four-wave-mixing processes in an optical fiber. The following question is asked - can stimulated Raman scattering be a mechanism by which adequate multiplicative stochastic phase fluctuations are introduced in the electric field of light undergoing four-wave-mixing as? Adequately checked numerical

algorithms of stimulated Raman scattering (SRS), spontaneous Raman generation and intrapulse Raman scattering (IRS) are used while exploring this issue. The algorithms are described in detail, as also are the results of the simulations. It is found that a 50-meter length of fiber (as used in the experiments), is too short to see the influence of Raman scattering, which is found to eventually dominate for longer fiber lengths.

In Chap. 4, self- and cross-phase modulation (XPM) of femtosecond pulses (~ 810 nm) propagating through a birefringent single-mode optical fiber (~ 6.9 cm) is studied both experimentally (using GRENOUILLE - Grating Eliminated No Nonsense Observation of Ultrafast Laser Light Electric Fields) and numerically (by solving a set of coupled nonlinear Schrödinger equations or CNLSEs). An optical spectrogram representation is derived from the electric field of the pulses and is linearly juxtaposed with the corresponding optical spectrum and optical time-trace. The effects of intrapulse Raman scattering (IRS) are discussed and the question whether it can be a cause of asymmetric transfer of pulse energies towards longer wavelengths is explored. The simulations are shown to be in good qualitative agreement with the experiments. Measured input pulse asymmetry, when incorporated into the simulations, is found to be the dominant cause of output spectral asymmetry. ² The results indicate that it is possible to modulate short pulses both temporally and spectrally by passage through polarization maintaining optical fibers with specified orientation and length. The modulation technique is very direct and straightforward. No frequency components of the broadband pulse have to be rejected as the entire spectrum is uniformly modulated. The technique is flexible as the modulation spacing can be varied by varying the fiber length.

²These averages are reported for 45 'detailed occupational codes', which is an intermediate occupational classification (between two and three-digit codes) given by the Current Population Survey (CPS).

Chapter 5 provides the conclusion to the thesis.

1.11 Theorems

Theorem 1.1 *This is my first theorem.*

1.12 Axioms

Axiom 1.1 *This is my first axiom.*

Axiom 1.2 *This is my second axiom in chapter 1.*

1.13 Tables

This is my table.

Table 1.1: Overview of test cases used in this study.

Test case	Quality variable (QV)	Setpoint for QV	Manipulated variables (MVs)
TE AZ	G/H ratio $x_B(H_2O)$	1.226	D-feed SP and Reactor Level SP Reflux flow and 5 th Tray temperature SP

My table is shown above. Normally it is double-spaced but I have inserted a command (marked in blue) to make it single-spaced and then inserted a command (again in blue) to change the text back to double-spacing.

1.13.1 Adding Extra Space between Text and Horizontal Lines

Table 1.2: Table with Extra Space between the Text and Horizontal Lines.

Test case	Quality variable QV	Setpoint for QV	Manipulated variables (MVs)
TE	G/H ratio	1.226	D-feed SP and Reactor Level SP
AZ	$x_B(H_2O)$		Reflux flow and 5 th Tray temperature SP

The line

```
\usepackage{tbls}
```

must be inserted in the preamble of your document. The table is set up to be single-spaced by

```
\renewcommand{\baselinestretch}{1} \small\normalsize
```

before

```
\begin{table}
```

. I set the first, second, and fourth columns as paragraphs, .5in, 1in, and 2.25in wide, respectively.

I then adjusted the separation between the words and the horizontal lines to 5ex by also adding

```
\setlength{\tablinesep}{5ex}
```

before the

```
\begin{table}
```

command.

After typing the table I change the document to be double-spaced from this point on.

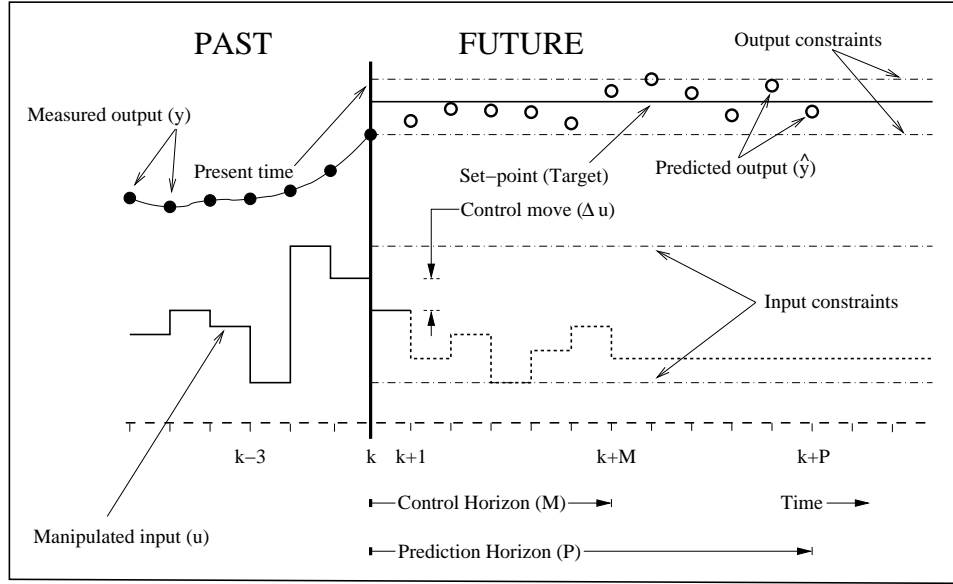


Figure 1.1: This figure caption is indented and single-spaced. Comparison between the experimental measurements [?] (black), the random initial condition NLSE model excluding phase noise (dashed curves) and the stochastic phase noise NLSE model (solid curves) showing the first- and second-order sideband evolution as a function of fiber length for $P_0 = 5.5 \text{ W}$, $\Omega = 366 \text{ GHz}$, $\Delta\nu = 0.5 \text{ GHz}$, $\gamma = 0.019 \text{ W}^{-1}\text{m}^{-1}$, and $\beta^{(2)} = 55 \text{ ps}^2/\text{km}$: dynamical evolution of the: (a) power in the first-order blue-shifted sideband, (b) power in the first-order red-shifted sideband, (c) fluctuations in the first-order blue-shifted sideband, (d) fluctuations in the first-order red-shifted sideband, (e) power in the second-order blue-shifted sideband, (f) power in the second-order red-shifted sideband.

1.14 Figures

The figure on the following page is centered and the figure caption is indented and single-spaced. Make sure you copy the last two lines

`\renewcommand{\baselinestretch}{2}\`

`\small\normalsize`

to return to double-spacing of your text.

The first figure is Fig.1.1. Please note that the figure label should be placed inside the figure

caption.

The next figure is placed landscape. It is Fig. [1.2](#).

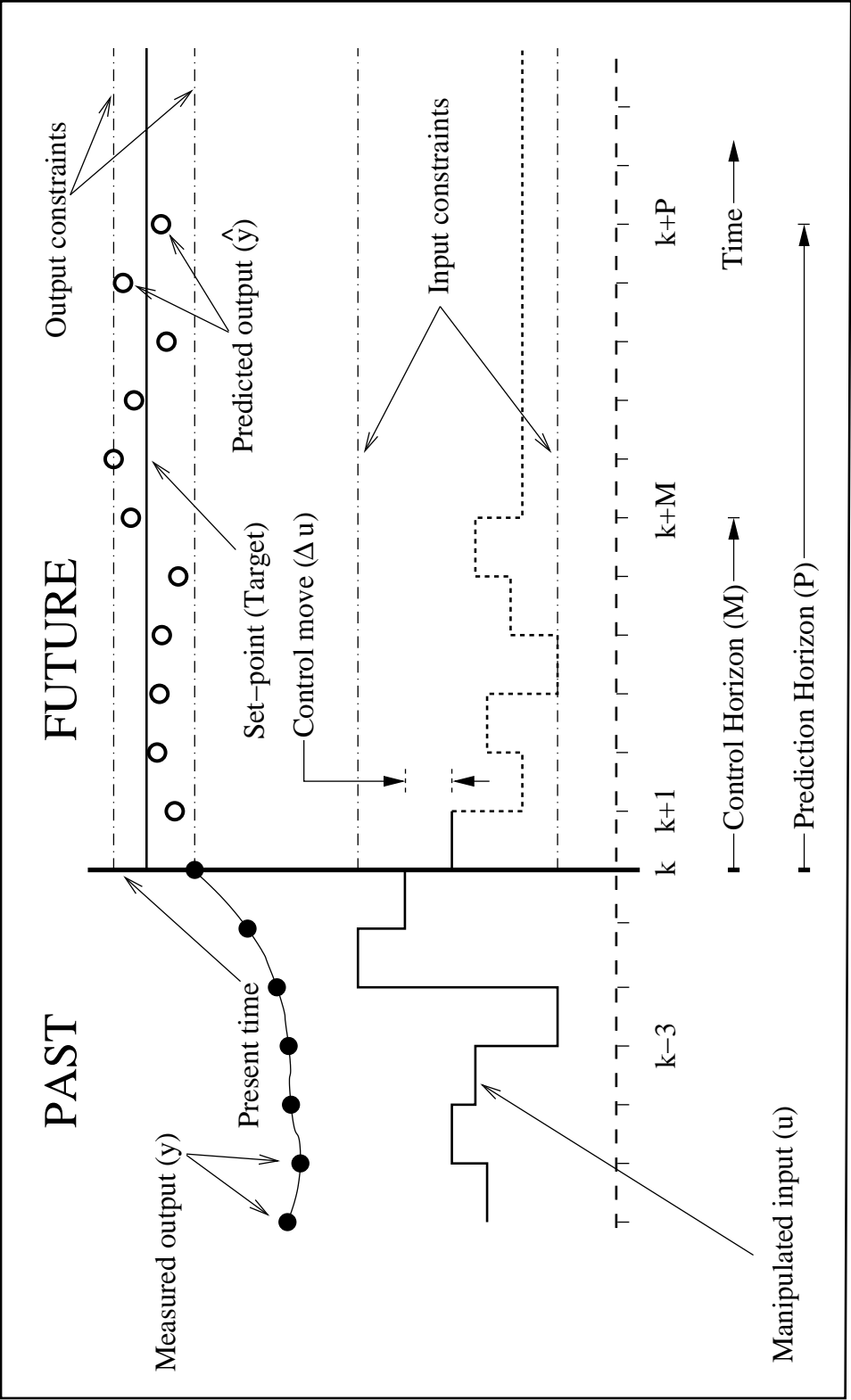


Figure 1.2: Schematic illustrating receding horizon control.

This is a my second figure which was placed landscape. Although I have used the same figure, I have renamed the label to fig:mpc-1. The second figure now becomes Figure [1.3](#).

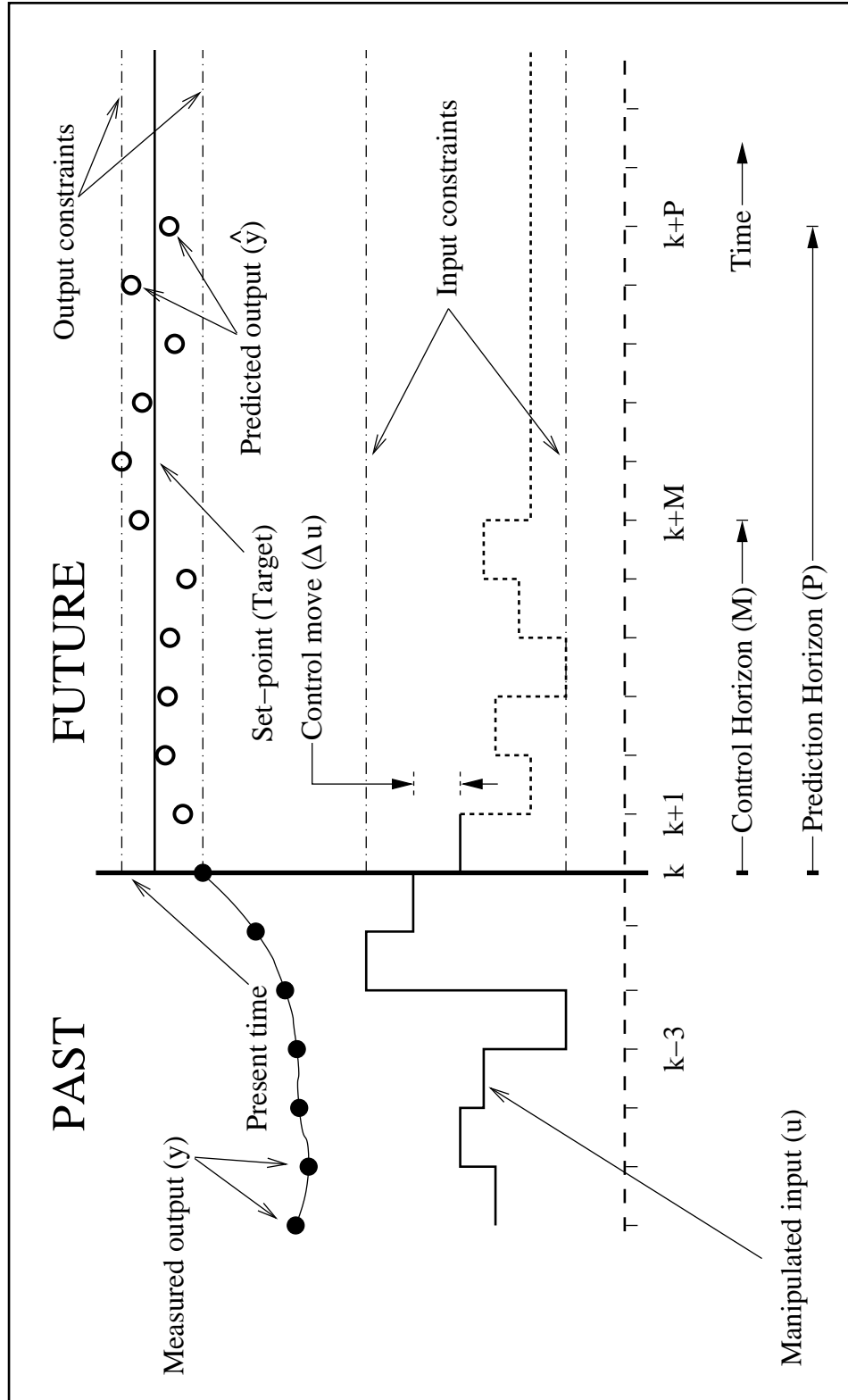


Figure 1.3: Schematic illustrating receding horizon control.

The following is an example of three subfigures with their figure captions and one single caption defining the three subfigures.

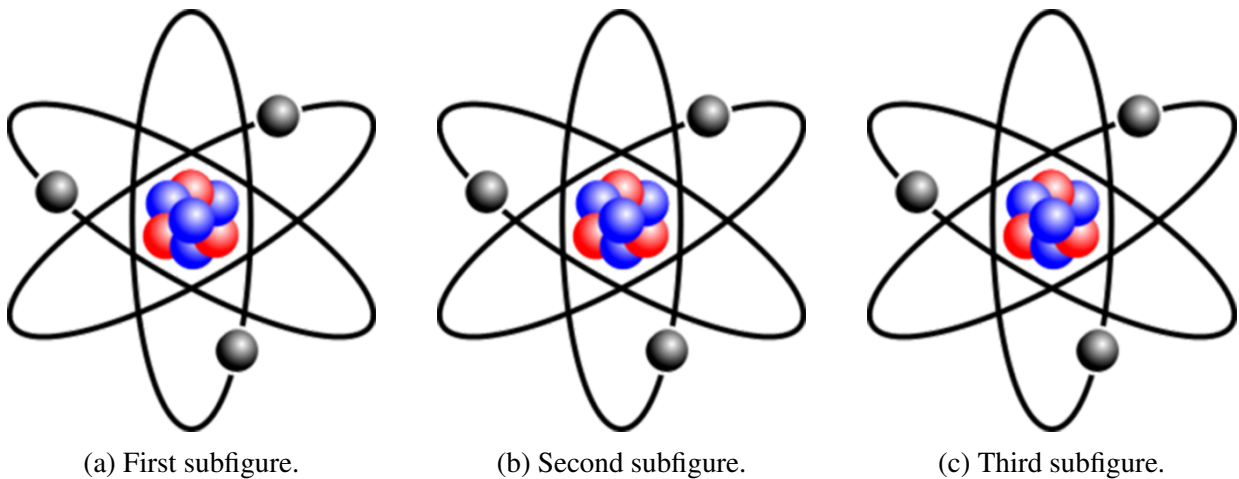


Figure 1.4: Creating subfigures in \LaTeX .

1.14.1 Numbering Figures

If you wish your figures to be numbered 1-100 without any reference to the chapter (e.g., Figure 1.1, 2.1, etc.), change the first line of your mainthesis.tex file to read

```
"\documentclass[12pt]{thesis-2}".
```

1.14.1.1 This is a Subsubsection

This is my first subsubsection in Chapter 1.

1.15 Short Titles in the Table of Contents, List of Figures, or List of Tables

The Table of Contents, List of Figures, or List of Tables usually show the entire title of a section, subsection, etc. or table, or the entire caption of a figure. If you put a short title in square

brackets after

```
\section, \table, or \figure,
```

the short title will show in your Table of Contents or lists.

```
\section[Short Title]{Title of Section}  
\subsection[Short Title]{Title of Subsection}
```

or when using a caption in a figure or table

```
\caption[Short Caption]{Full text of the caption.}
```

1.16 Figures on Text Page

Normally figures in the thesis are placed on a page by themselves. The following figure is placed on the page with text before and after the figure by adding `[!!h]` after

```
\begin{figure}[!!h]
```

. Please note that the figure label is placed within the caption.

```
\begin{figure}[!!h]  
  \begin{center}  
    \includegraphics[width=5in]{mpc.eps}  
  \end{center}  
  \caption[Short title]{Schematic illustrating receding horizon control.  
  \label{fig:mpc-2}}  
\end{figure}
```

This does not necessarily mean that the text before and after the figure will be exactly what you want. Remember Latex will place the figure where it will fit on the page the best. The previous figure is Figs. [1.5](#).

1.17 Wrapping Text around Figure

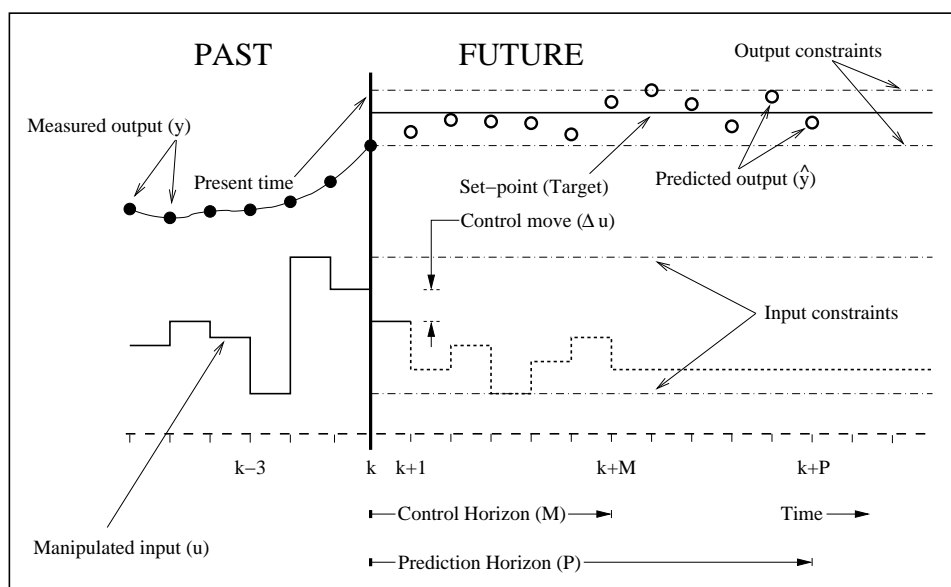


Figure 1.5: Schematic illustrating receding horizon control.

By way of summary, at the end of the activity, I reminded the class of what we'd done: by considering relatively nearby galaxies whose distance we had measured by some other means, we were able to establish a relationship locally between redshift and distance. By way of summary, at the end of the activity, I reminded the class of what we'd done: by considering relatively nearby galaxies whose distance we had measured by some other means, we were able to establish a relation-

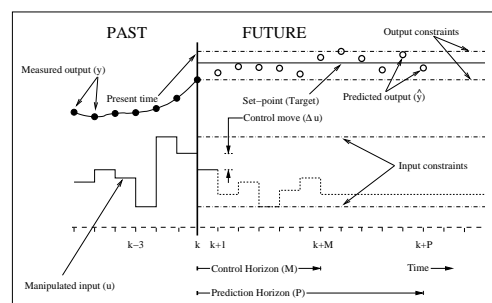


Figure 1.6: Text wrap around figure. Text wrap around figure. Text wrap around figure. Text wrap around figure. Text wrap around figure. Text wrap around figure.

ship locally between redshift and distance. By way of summary, at the end of the activity, I reminded the class of what we'd done: by considering relatively nearby galaxies whose distance we had measured by some other means, we were able to establish a relationship locally between redshift and distance. By way of summary, at the end of the activity, I reminded the class of what

we'd done: by considering relatively nearby galaxies whose distance we had measured by some other means, we were able to establish a relationship locally between redshift and distance. See Fig. 1.6.

1.18 LaTeX – A Typesetting Program

A 13-page explanation of some of the features of LaTeX can be downloaded from <http://www.jgsee.kmutt.a>

1.19 Using Bibtex

Using Bibtex with Latex documents is not difficult. The bulk of the work is organizing your bibtex file, which is a data base compiled by you of the articles, books, etc. which you use in the bibliographies or reference sections of your publications.

I have linked several files to this webpage, which will be helpful when you are using Bibtex. These files can be downloaded from

<http://www.ireap.umd.edu/ireap/theses/bibtex>. Please read the file "BibtexInstructions.pdf". The first two pages explain how to set up and run Bibtex; the remaining pages were taken from a published article and show how the references were cited in the .tex file. The files

BibtexInstructions.tex, Galactic.bib, Dottie.bib are the original .tex files used for

BibtexInstructions.pdf. The file BibtexSamples.tex contains examples of the information needed for the various publications you wish to reference (e.g., articles in refereed journals, books, unpublished articles, conference proceedings, etc.).

If you have questions concerning Bibtex, please contact me at 301-405-4955 or dbrosius@umd.edu.

1.20 Using Natbib

Another option of citing references in the bibliography is using Natbib instead of Bibtex. You must still create a bibtex file, as noted above. The command "backslash cite" cannot be used with natbib; instead "backslash citet" and "backslash citep" must be used. "backslash citet" is used to show references in the text (e.g., Eq. 8 in Reiser,1996 shows ...); "backslash citep" is used in the parenthetical (e.g., Eq. 8 (Reiser, 1996) shows ...).

Add in preamble -- `\usepackage[option]{natbib}` -- A list of options to be used with Natbib can be found at "<http://merkel.zoneo.net/Latex/natbib.php>".

Add at bottom of mainthesis.tex file --

```
\bibliography{name of your bibtex file}
```

```
\bibliographystyle{plainnat, abbrnat, or unsrtnat} (I usually use  
unsrtnat)
```

Typesetting: pdf_latex, Bib, pdf_latex, pdf_latex

I use MikTeX with WinEdt.

The reference sheet for natbib usage can be found at "<http://merkel.zoneo.net/Latex/natbib.php>".

1.21 APS Physical Review Style and Notation Guide

The following style guide may be downloaded from The American Physical Society at <http://forms.aps.org/author/styleguide.pdf>: Physical Review Style and Notation Guide, published by The American Physical Society, compiled and edited by Anne Waldron, Peggy Judd, and Valerie Miller, February 1993. It may be old, but it is very useful.

Bibliography